ACS OMEGA

Open Access

This article is licensed under CC-BY-NC-ND 4.0

http://pubs.acs.org/journal/acsodf

Article

A DFT Study of the Reaction Products/Mechanism in Plasma-Assisted Ammonia Synthesis from Water and Nitrogen and Their Infrared Analysis

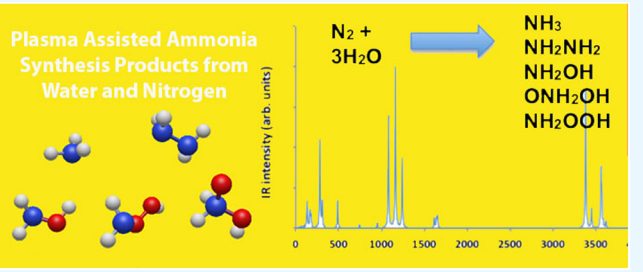
Constantinos D. Zeinalipour-Yazdi* and Xinyan Wang

Cite This: https://doi.org/10.1021/acsomega.6c03586

Read Online

ACCESS | Metrics & More | Article Recommendations

ABSTRACT: This paper presents a thorough investigation of potential reaction products when water and nitrogen react in the gas phase and a reaction mechanism is proposed. We present thermochemistry and simulated infrared (IR) spectroscopy of reactions involved in the synthesis of ammonia (NH_3), hydrazine (N_2H_4), and some new ammonia-based molecules (NH_2OOH, ONH_2OH) from water (H_2O) and nitrogen gas (N_2). The production of ammonia and hydrazine is of significant interest because of their essential roles as chemical feedstocks, propellants, and potential clean energy carriers. However, the underlying chemical processes and their energy requirements have not been fully explored, especially considering the environmental effects of their use as fuels in internal combustion engines (ICE). We find that there are 6 different reaction products that may be formed during the ammonia synthesis from N_2 and H_2O, which include ammonia, hydrazine, hydroxylamine (NH_2OH), ammonia oxide ($NH_3^+-O^-$), and two forms of hydroxylamine oxide (NH_2OOH, ONH_2OH), and the latter chemical species have not been previously reported or synthesized. The partially oxidized products of ammonia have similar formation energies to those of ammonia, which suggests that they could be produced during the plasma-assisted synthesis. Our simulated infrared spectra can help in the identification and characterization of ammonia synthesis products.



1. INTRODUCTION

Global warming is a reality in certain regions of the globe, which requires immediate action. Since the Paris Agreement (Dec 12, 2015) at the 21st Conference of the Parties to the United Nations Framework Convention on Climate Change (COP21) aimed to achieve net-zero emissions in the second half of the century, there have been significant efforts by the scientific community to find fuels that do not produce CO_2 when oxidized.[1] CO_2 is a major greenhouse gas and contributes to global warming, and since the Industrial Revolution (1850−2019), 2.4 trillion tons of CO_2 have been emitted, raising the global average temperature by 1.07 °C.[1]

The suggestion of using ammonia as a fuel in internal combustion engines (ICE) was first implemented in WWII, when ammonia-fueled buses were produced in Belgium (1943).[2] In fact, it has been shown that ammonia can be used in ICE as a fuel, with only minor modifications to the engine.[2] Recently, it has been suggested that ammonia could be a fuel for maritime transport as an effort to reach net-zero emissions in the shipping industry.[3,4] As the energy capacity of stored liquid ammonia is greater than that of liquid hydrogen (see Table 1 from ref 5), and the storage and transportation of liquid hydrogen is challenging, it has been suggested that ammonia may be an alternative fuel carrier that poses lower risks.[6]

Furthermore, ammonia use as a fertilizer suggests that its distribution network is already in place around the world.[7] Nevertheless, because 50% of the global production of ammonia relies on fossil fuels, and this is going to increase if it is also used as a fuel, more sustainable methods of producing ammonia are desirable. We have previously suggested new mechanisms[8] on the basis of DFT calculations for the synthesis of ammonia via methods that utilize nitrogen vacancies on metal nitrides such as Co_3Mo_3N[9−11] and Fe_3Mo_3N.[12] Also, chemical looping methods for the medium-scale synthesis of ammonia have been suggested by us.[13] Industrially, ammonia is currently synthesized from dinitrogen and molecular hydrogen via the Haber−Bosch process (H−B). This process uses an iron potassium oxide promoted catalysts ($Fe-K_2O-Al_2O_3$), which operate at high temperatures (400−500 °C) and

Received: May 14, 2026
Revised: August 11, 2026
Accepted: August 11, 2026

ACS Publications

© XXXX The Authors. Published by American Chemical Society

Downloaded from pubs.acs.org/acsodf/article-pdf/doi/10.1021/acsomega.6c03586/6768896/acsomega.6c03586.pdf by Constantinos Zeinalipour-Yazdi on 29 August 2026

Table 1. Comparison of Energy (Megawatt-Hour) per Unit Volume (m^3) of Ammonia and Hydrogen[a]

liquid ammonia	hydrogen at 1 bar, 300 K	hydrogen at 300 bar, 300 K	hydrogen at 700 bar, 300 K	liquefied hydrogen
3.58 MWh/m^3	0.003 MWh/m^3	0.67 MWh/m^3	1.34 MWh/m^3	2.3 MWh/m^3

[a]Reprinted in part with permission from Serpell, O.; Hsain, Z.; Chu, A.; and Johnsen, W., Ammonia's role in net-zero hydrogen economy, Kleinman Center of Energy Policy, March 2023.[5]

pressures (100−200 atm).[14] The source of N_2 is atmospheric air, whereas H_2 is produced from steam reforming[15] in which methane (CH_4) is reacted with steam at elevated temperatures/pressures (850 °C and 2.5 × 10^6 Pa), producing carbon monoxide (CO) and H_2 according to the reaction

$$CH_4(g) + H_2O(g) \Rightarrow CO(g) + 3H_2(g) \quad (1)$$

Subsequently, the water−gas shift reaction[16] is utilized, where more hydrogen is produced by reacting CO and steam using a nickel catalyst to produce carbon dioxide and more hydrogen according to the reaction

$$CO(g) + H_2O(g) \Rightarrow CO_2(g) + H_2(g) \quad (2)$$

Between 1.8 and 2.1 tons of CO_2 are emitted for every ton of NH_3 synthesized by the Haber−Bosch process.[17] This means that currently ammonia has a significant carbon footprint, which accounts for 2% of the global energy supply, if we only consider its use as a fertilizer.[18]

In order to produce ammonia as a net-zero fuel, the H_2 would have to originate from a renewable energy source, such as H_2 produced by water electrolysis, which is powered by photovoltaics.[19] This is especially feasible by the use of cheap, flexible, and transparent carbon-based photovoltaics[20] that are currently produced and that can coat windows and rooftops in cities that do not require additional land to be purchased or rented.[21]

Complete combustion of ammonia under ideal conditions produces environmentally friendly gases such as water and dinitrogen according to the following reaction

$$4NH_3(g) + 3O_2(g) \Rightarrow 2N_2(g) + 6H_2O(g) \quad (3)$$

However, at elevated temperatures of combustion, it is expected to also produce some nitrogen oxides, NO_x (e.g., nitrous oxide, N_2O, nitrogen monoxide, NO, and nitrogen dioxide, NO_2).[22,23] These nitrogen oxides are harmful gases and, when they are low in the atmosphere, can significantly affect human health and the environment. Mainly by irritating the airways in the human respiratory system, causing asthma, which leads to coughing, wheezing, and difficulty breathing.[22] Children and the elderly are in particular vulnerable to elevated levels of nitrogen oxides in the atmospheric air in populated areas. Additionally, nitrogen oxides, when dissolved in rainwater, cause acid rain, which affects aquatic life in lakes and other sensitive ecosystems such as forests and crops. A nonreversible effect of acid rain is the gradual degradation of archeological monuments, marble, and limestone that contain calcite (i.e., calcium carbonate, $CaCO_3$), as shown in eq 4

$$CaCO_3(s) + 2HNO_3(aq) \Rightarrow Ca(NO_3)_2(aq) + CO_2(g) + H_2O(l) \quad (4)$$

It has been suggested that nitrogen oxides can be reduced in the ICE exhaust by using a NO_x scrapper, which is a catalyst that converts NO_x to environmentally friendly gases such as N_2 and O_2.[24] Currently, there are various deNO_x technologies available for exhaust gas aftertreatment that use ammonia, such as the selective catalytic reduction (SCR) shown in eq 5[25,26]

$$4NO(g) + 4NH_3(g) \Rightarrow O_2(g) + 4N_2(g) + 3H_2O(g) \quad (5)$$

Ammonia has therefore emerged as a crucial player in the quest for cleaner, more sustainable energy solutions. Its significance as a fuel cannot be understated, as it offers a unique set of attributes that position it at the forefront of efforts to reduce greenhouse gas emissions. It has therefore been desirable to find new methods of producing NH_3 from reactions of molecules that are available to us in nature. One such method has been the suggestion to produce ammonia from dinitrogen from air and water over a catalyst.[27] It has also been previously suggested that ammonia can be synthesized in an electrochemical cell from water and nitrogen.[28] Another popular emerging method employed to study the synthesis of ammonia with the use of plasma (i.e., energetic electrons) has been shown to enhance the reaction rate for ammonia synthesis from nitrogen and hydrogen over various metal hydrides and other catalytic materials.[29−36]

In this study, we performed all-electron DFT calculations with the B3LYP functional and Dunning's spherical augmented correlation consistent polarized valence double-ζ basis set, denoted as aug-cc-pVDZ(5d, 7f)[37] to understand the thermodynamics of various reactions that lead to the formation of fuels such as ammonia (NH_3), hydrazine (NH_2NH_2), hydroxylamine (NH_2OH), and hydroxylamine oxide (NH_2OOH, ONH_2OH). We have also simulated the infrared (IR) absorption spectra of the various reaction pathways examined and provided a unique recipe to help spectroscopists to differentiate between the various formed products that are produced during the synthesis of ammonia under plasma conditions. Lastly, we propose a mechanism for the plasma-assisted ammonia synthesis from water and nitrogen.

2. COMPUTATIONAL METHODS

We have optimized fully with the B3LYP/aug-cc-pVDZ(5d, 7f) method various reaction pathways for the formation of ammonia and hydrazine.[38,39] All calculations were done in Gaussian 16.[40] Finding the various reaction pathways for the formation of ammonia and hydrazine requires chemical intuition, many starting structures, and careful observation of the product structures. Some starting structures result in the same product and can therefore not be attributed to a new reaction pathway. We have tried many reaction products that hold the stoichiometry of the reactants, having 2 nitrogen atoms, 6 hydrogen atoms, and three oxygens constructing the product molecules. The overall charge of the reaction was kept neutral, and this reduces the possible pathways available. Vibrational analysis confirmed that the molecules found are minima of the potential energy surface and that they are potential products formed during the synthesis. The simulated infrared spectra are provided for their identification.

Downloaded from pubs.acs.org/acsodf/article-pdf/doi/10.1021/acsomega.6c03586/6768896/acsomega.6c03586.pdf by Constantinos Zeinalipour-Yazdi on 29 August 2026

https://doi.org/10.1021/acsomega.6c03586
ACS Omega XXXX, XXX, XXX−XXX

Table 2. Tabulated Values of Various Reaction Pathways Found and Their Corresponding Energy Changes (ΔE_{rxn}), Enthalpy Changes (ΔH_{rxn}), and Gibbs Free Energy Changes (ΔG_{rxn})[a]

pathway	reaction	ΔE_{rxn}	ΔH_{rxn}	ΔG_{rxn}
1	$N_2 + 3H_2O \rightarrow 2NH_3 + O_3$	776.8	779.3	793.8
2	$N_2 + 3H_2O \rightarrow NH_3 + NH_3O + O_2$	776.6	788.6	817.3
3	$N_2 + 3H_2O \rightarrow NH_2NH_2 + O_2 + H_2O$	690.2	702.9	713.2
4	$N_2 + 3H_2O \rightarrow NH_2OH + O_2 + NH_3$	756.1	762.9	785.9
5	$N_2 + 3H_2O \rightarrow NH_2OH + ONH_2OH$	563.9	582.2	618.3
6	$N_2 + 3H_2O \rightarrow NH_2OH + NH_2OOH$	682.8	693.0	717.1

[a]All energy values given in kJ·mol^{-1} are values calculated at T = 298.15 K and P = 1 atm.

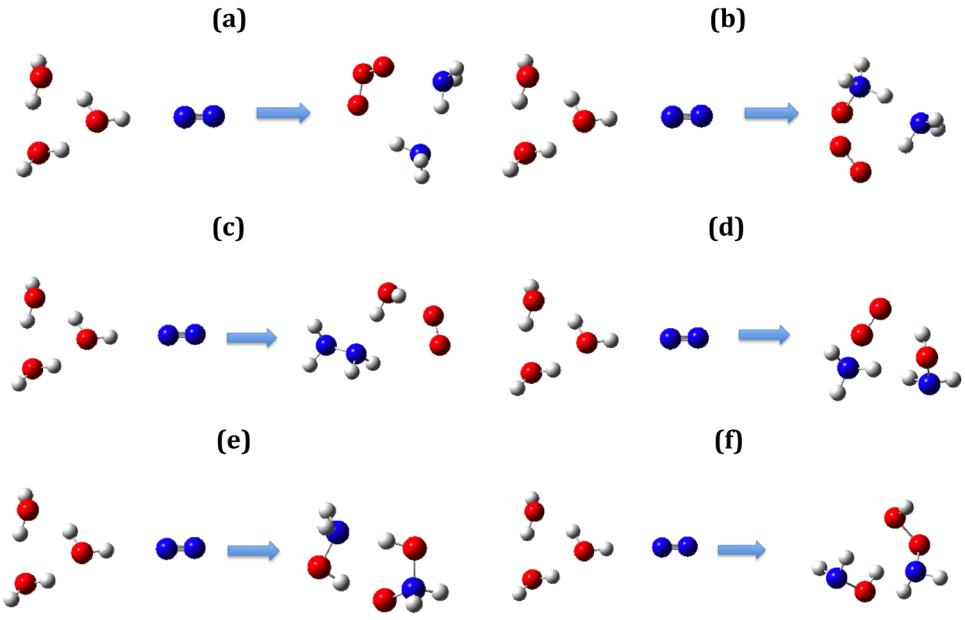


Figure 1. (a) Optimized structures at B3LYP/aug-cc-pVDZ(5d, 7f) level of theory of the reaction: $N_2 + 3H_2O \rightarrow 2NH_3 + O_3$ (pathway 1), (b) $N_2 + 3H_2O \rightarrow NH_3 + NH_3O + O_2$ (pathway 2), (c) $N_2 + 3H_2O \rightarrow NH_2NH_2 + O_2 + H_2O$ (pathway 3), (d) $N_2 + 3H_2O \rightarrow NH_2OH + O_2 + NH_3$ (pathway 4), (e) $N_2 + 3H_2O \rightarrow NH_2OH + ONH_2OH$ (pathway 5), and (f) $N_2 + 3H_2O \rightarrow NH_2OH + NH_2OOH$ (pathway 6).

3. RESULTS AND DISCUSSION

3.1. Thermochemistry of the Reaction of N_2 and H_2O

In the following section, we provide a table with the various reaction pathways found and their corresponding reaction energy changes (ΔE_{rxn}), enthalpy changes (ΔH_{rxn}), and Gibbs free energy changes (ΔG_{rxn}). We find a total of 6 reaction pathways that result in drastically different products, including ammonia (NH_3), hydrazine (NH_2NH_2), hydroxylamine (NH_2OH), and hydroxylamine oxide (NH_2OOH, ONH_2OH). These results are shown in Table 2.

The general pathways for the formation of ammonia that we find are

$$\text{pathway 1: } N_2\,(g) + 3H_2O\,(g) \rightarrow 2NH_3\,(g) + O_3\,(g) \quad (6)$$

$$\text{pathway 2: } N_2(g) + 3H_2O\,(g) \rightarrow NH_3(g) + NH_3O\,(g) + O_2\,(g) \quad (7)$$

In pathway 1 (shown in Figure 1), three water molecules in a cyclic H-bonded cluster interact with dinitrogen via the O−H group pointing into the negatively charged lone electron pair orbital of N_2. This is the global minimum for these reactants, but in a gas mixture of the two gases, many other local minima are possible, and therefore, the reaction pathways are many. Therefore, we have not explored reaction barriers but just the starting (reacting) molecules and their products that maintain the stoichiometry of the reaction. In this first reaction pathway, the products are two ammonia molecules that are H-bonded and the ozone (O_3) molecule. The fact that ozone is a product is interesting and requires further investigation, as ground-level ozone (i.e., tropospheric) is an air pollutant in comparison to stratospheric ozone, where it acts as a UV filter, absorbing mostly UV−B radiation. The Gibbs free energy change for this reaction is 793.8 kJ·mol^{-1}, which indicates that it is a very endergonic reaction.

The second reaction pathway (shown in Figure 1b) considered is one in which oxygen (O_2), ammonia, and NH_3O are formed. Here, the stoichiometric amount of ammonia is only half as large compared to the first pathway, but interestingly, we have the formation of NH_3O, which could also be a potential nitrogen-containing fuel, which is, however, partially oxidized. This suggests that the heat content of this fuel is reduced, but if we look at the Gibbs free energy change of this reaction, we find that it is even higher than the first pathway, being endergonic by 817.3 kJ/mol. This is due to the formation of O_2 rather than O_3 and suggests that the second pathway produces a fuel that has fuel values similar to pathway

Downloaded from pubs.acs.org/acsodf/article-pdf/doi/10.1021/acsomega.6c03586/6768896/acsomega.6c03586.pdf by Constantinos Zeinalipour-Yazdi on 29 August 2026

https://doi.org/10.1021/acsomega.6c03586
ACS Omega XXXX, XXX, XXX−XXX

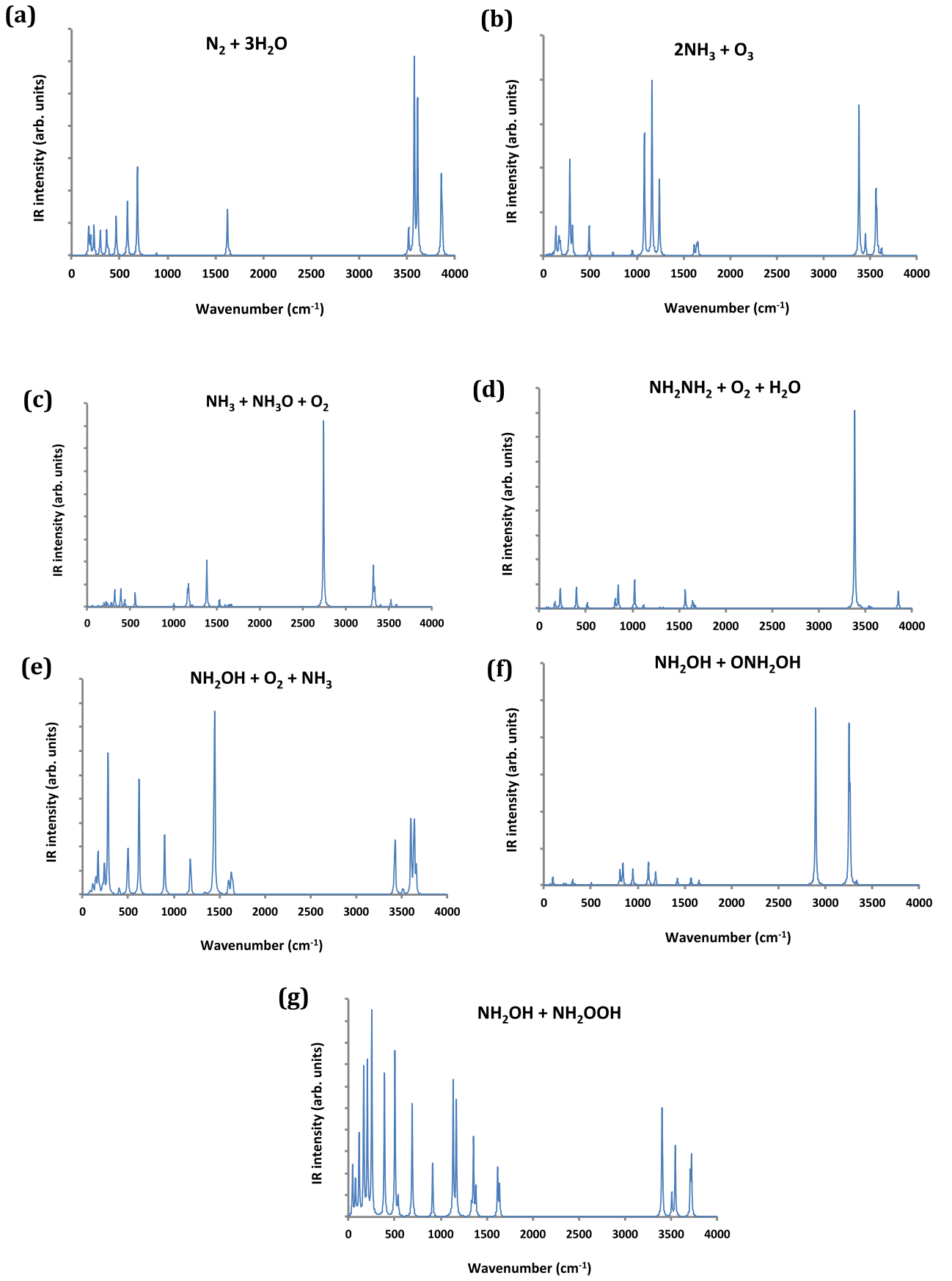


Figure 2. Simulated IR spectrum using B3LYP//aug-cc-pVDZ(5d, 7f) of the (a) $3H_2O + N_2$ model shown in Figure 1a, (b) $2NH_3 + O_3$ model shown in Figure 1b, (c) $NH_3 + NH_3O + O_2$ model shown in Figure 1c, (d) $NH_2NH_2 + O_2 + H_2O$ model shown in Figure 1d, (e) $NH_2OH + O_2 + NH_3$ model shown in Figure 1e, (f) $NH_2OH + ONH_2OH$ model shown in Figure 1f, and (g) $NH_2OH + NH_2OOH$ model shown in Figure 1g.

Downloaded from pubs.acs.org/acsodf/article-pdf/doi/10.1021/acsomega.6c03586/6768896/acsomega.6c03586.pdf by Constantinos Zeinalipour-Yazdi on 29 August 2026

https://doi.org/10.1021/acsomega.6c03586
ACS Omega XXXX, XXX, XXX−XXX

1. It is conceivable that the net-zero fuel may not necessarily be ammonia, but some oxidized product of ammonia if the fuel value of this molecule is still high. We show later that there are some oxidized products of ammonia that have very high Gibbs free energies of formation, which suggests that they have a large fuel value. These molecules have not been previously reported in the literature and thus should be considered in the future searches for ammonia-based fuels.

The third reaction pathway (shown in Figure 1c) that we investigated was the one that leads to the formation of hydrazine (NH_2NH_2), which is known to be a rocket fuel. Hydrazine is known to be an intermediate in the direct gas-phase hydrogenation of N_2, as we have previously shown via DFT calculations.[41] In this reaction pathway, one water molecule remains unreacted and only the hydrogens from two water molecules, hydrogenate dinitrogen, forming hydrazine. This reaction pathway is given by

$$\text{pathway 3: } N_2\,(g) + 3H_2O\,(g) \rightarrow NH_2NH_2\,(g) + O_2(g) + H_2O\,(g) \quad (8)$$

It is expected that during the formation of ammonia in the first two pathways explored, there will also be some formation of hydrazine due to pathway 3. This reaction pathway is endergonic by 713.2 kJ·mol^{-1}, which is about 92 kJ·mol^{-1} lower than the first two pathways that produce ammonia. This implies that the energy content of a nitrogen-based fuel that also contains hydrazine would be smaller than the one that is pure in ammonia. Furthermore, the reaction in pathway 3 also produces $O_2(g)$, which is known to oxidize hydrazine to water and nitrogen, as hydrazine is used to remove trace amounts of $O_2(g)$ from aqueous solutions.[42]

The fourth reaction pathway (shown in Figure 1d) investigated is very similar to reaction pathway 2. Here, we observe the formation of only half the stoichiometric amount of ammonia, oxygen, and a structure of hydroxylamine (NH_2OH), which is thermodynamically more stable than NH_3O formed in pathway 2. However, hydroxylamine is difficult to store as it is an unstable molecule. This reaction pathway is given by

$$\text{pathway 4: } N_2\,(g) + 3H_2O\,(g) \rightarrow NH_2OH\,(g) + O_2\,(g) + NH_3(g) \quad (9)$$

This can be seen in the relative Gibbs free energy changes of pathway 2 and pathway 4, which differ by about 31 kJ·mol^{-1}.

The fifth reaction pathway (shown in Figure 1e) investigated results in the formation of hydroxylamine (NH_2OH) and hydroxylamine oxide (ONH_2OH), which can both be considered as partially oxidized products of ammonia. This pathway has the reaction

$$\text{pathway 5: } N_2\,(g) + 3H_2O\,(g) \rightarrow NH_2OH\,(g) + ONH_2OH\,(g) \quad (10)$$

This is evident by the energy change for this reaction, which is about 187 kJ/mol less endergonic than reaction pathways 1 and 2, which result in the formation of ammonia. This can be attributed to the fact that the products of this reaction have −OH and −OOH functional groups, which indicate various stages of oxidation of the amines.

There is also a sixth pathway (shown in Figure 1f) for the reaction of water with nitrogen that results in the formation of NH_2OH and NH_2OOH, given by

$$\text{pathway 6: } N_2\,(g) + 3H_2O\,(g) \rightarrow NH_2OH\,(g) + NH_2OOH\,(g) \quad (11)$$

This reaction pathway is endothermic by 693.0 kJ·mol^{-1} and endergonic by 717.1 kJ·mol^{-1} and results in the formation of hydroxylamine oxide (NH_2OOH), which has yet to be isolated experimentally, to the best of our knowledge. This molecule still has a very high Gibbs free energy of formation, similar to ammonia, which indicates that it will also have a high fuel value based on the thermodynamic properties listed in Table 2. We suggest that this molecule should be further explored experimentally in search of ammonia-based net-zero fuels. This molecule has a hydroperoxy functional group (−OOH), which could make it a better fuel as the oxidizing group is already in contact with the molecule. There is no reference in the literature to the best of our knowledge about the synthesis of this molecule, but our calculations show that it is a stable molecule with relatively high fuel values, on the basis of Gibbs free energy calculations.

We observe that the reaction of N_2 and water results in 6 different reaction products, all of which contain net-zero fuels, given that the H_2 is produced in a renewable way. Some of these products may emit less NO_x and may be synthesized more easily. What is noteworthy is that even the partially oxidized products of ammonia have very high fuel values, judging from the Gibbs free energy of the reaction given in Table 2. It would therefore be interesting to study the combustion rate of these products through adiabatic bomb calorimetry coupled to mass spectrometry to look at the reaction products and the rate of combustion. In the following section, we perform IR spectroscopic identification of the various reaction products and reactants for ammonia synthesis from water and nitrogen.

3.2. Simulated IR Spectra of Reaction Products

We provide a detailed analysis of the simulated IR spectra of the reactants and products of the ammonia, hydrazine, and oxidized products of ammonia synthesis reaction from water and dinitrogen. The analysis of the simulated IR spectra is given from high wavenumbers (i.e., 4000 cm^{-1}) to low wavenumbers (i.e., 0 cm^{-1}).

In Figure 2, we present the simulated IR spectrum of all optimized reactants and products shown in Figure 1. For the reactants of the reaction at 3858 cm^{-1}, we observe the stretching vibration of the O−H of water that interacts with dinitrogen (shown in Figure 2a). In a triple peak that ranges between 3517 and 3612 cm^{-1}, we observe the other O−H stretching vibrations that are due to H-bonded networks in water. The bending vibration of water appears at 1628 cm^{-1}. The out-of-plane wagging vibrations of water appear between 687 and 176 cm^{-1}. The stretching vibration of the N−N bond appears at 67 cm^{-1}.

In Figure 2a, we present the simulated IR spectrum of the products of pathway 1 shown in Figure 1a. For the products of this reaction, which are ammonia and ozone shown in Figure 2b, the IR peaks appearing at high wavenumbers are as follows: At 3570 cm^{-1}, we see the stretching vibration of the N−H bond of NH_3. At 3379 cm^{-1}, we observe the stretching vibration of H-bonded N−H with adjacent ammonia

Downloaded from pubs.acs.org/acsodf/article-pdf/doi/10.1021/acsomega.6c03586/6768896/acsomega.6c03586.pdf by Constantinos Zeinalipour-Yazdi on 29 August 2026

https://doi.org/10.1021/acsomega.6c03586
ACS Omega XXXX, XXX, XXX−XXX

molecules. This is expected as H-bonded N−H will have a lower bond strength and therefore lower force constant and consequently lower vibrational wavenumber. At 1639 cm^{-1}, a very low intensity peak that corresponds to the bending vibration of H−N−H appears. Lower in wavenumber are two peaks that correspond to the stretching vibration of O−O in ozone, the first interacting with the N of ammonia (1240 cm^{-1}) and the second with the H of ammonia (1161 cm^{-1}). Between 1079 and 949 cm^{-1}, we observe the wagging motion of hydrogen in ammonia molecules. At 743 cm^{-1} is a very narrow peak that corresponds to the bending vibration of O_3. Below 487 cm^{-1}, we observe the rocking vibration of ammonia molecules.

By comparing the two IR spectra in Figure 2a,b, we have reached the conclusion that observation of the disappearance of the peak that corresponds to the O−H vibration (3858 cm^{-1}) of water that interacts directly with N_2 molecules is the most prominent spectral change that happens when forming ammonia in pathway 1, from water and dinitrogen.

In Figure 2c, we present the simulated IR spectrum of pathway 2 for the production of ammonia, NH_3O, and O_2 from H_2O and N_2. The highest wavenumber peak in this gas mixture is at 3521 cm^{-1}, which corresponds to the stretching vibration of NH_3. This peak is very weak and may not be observed experimentally. At 3319 cm^{-1}, there is another stretching vibration of the N−H bond that interacts with an O_2 molecule. This peak is of higher intensity than the previous one. However, the peak that has the highest intensity in this simulated IR spectrum is the peak that corresponds to the N−H vibration of H-bonded NH_3O with NH_3, which appears at 2741 cm^{-1}. At 1386 cm^{-1}, the stretching vibration of O_2 appears in a moderate in intensity peak. Lower in wavenumber, a very weak peak corresponds to the wagging motion of the hydrogen in ammonia. Below 554 cm^{-1}, there are other weak peaks that correspond to the bending of the hydrogen bond between NH_3 and NH_3O.

Comparing the IR spectrum of the reactants and products of this reaction, the peak at 2741 cm^{-1}, which corresponds to the stretching vibration of N−H H-bonded NH_3O with NH_3, can be used as an identifier that ammonia and NH_3O have been produced.

In Figure 2d, we present the simulated IR spectrum of NH_2NH_2, O_2, and H_2O, which are the products of pathway 3. The highest wavenumber peak (3852 cm^{-1}) in this spectrum is the asymmetric stretching vibration of the O−H bonds in water, which is very weak in intensity. The symmetric stretching vibration of H_2O is much lower in wavenumber and appears at 3384 cm^{-1}. The bending vibration of water appears at 1649 cm^{-1} in a very weak intensity peak. In the same region is the stretching vibration of O_2 (1566 cm^{-1}). At 1117 cm^{-1} is the stretching vibration of the N−N in hydrazine, overlapping with various twisting vibrations of the hydrogen of hydrazine. The latter peaks have very low intensities.

By comparing the spectra of the reactants and products of pathway 3, we reach the conclusion that the peak that corresponds to the symmetric stretching vibration of water (3384 cm^{-1}) that is hydrogen-bonded to N of hydrazine can be used as an identifier for the formation of the products (i.e., NH_2NH_2) of this reaction.

In Figure 2e, we present the simulated IR spectrum of the products of pathway 4, which are NH_2OH, O_2, and NH_3. The highest wavenumber peak in this spectrum is the antisymmetric stretching frequency of ammonia at 3648 cm^{-1}. In the same region of the spectrum is the stretching vibration of the O−H in NH_2OH (3626 cm^{-1}, moderate) and another antisymmetric stretching vibration of ammonia (3592 cm^{-1}, moderate), whereas the symmetric stretching vibration of ammonia appears lower in wavenumber, at 3417 cm^{-1}. At 1639 cm^{-1} is the bending vibration of the H−N−H moiety in NH_2OH and ammonia. A very intense peak corresponds to the stretching vibration of O_2, which appears at 1436 cm^{-1}.

By comparing the spectra that correspond to the products and reactants of pathway 4, we reach the conclusion that the formation of the products can be monitored by looking at the O−O stretching vibration peak at 1436 cm^{-1}, which is the most intense peak in the simulated IR spectrum.

In Figure 2f, we present the simulated IR spectrum of the products of reaction pathway 5, which are NH_2OH and ONH_2OH. The highest wavenumber peak in this spectrum is the stretching vibration of the O−H of NH_2OH (3263 cm^{-1}, very intense), which is H-bonded to an adjacent ONH_2OH molecule. Somewhat lower in wavenumber is the stretching vibration of O−H in ONH_2OH (2895 cm^{-1}, very intense), which is also H-bonded to an adjacent NH_2OH molecule. At 1420 cm^{-1}, we observe a very weak peak that corresponds to the wagging motion of the hydrogens of the molecules NH_2OH and ONH_2OH. The stretching wavenumber of the N−O bond in ONH_2OH appears at 1112 cm^{-1}, which is also a very weak intensity peak.

Comparison of the simulated IR spectrum of the reactants and products of pathway 5, we reached the conclusion that the products of this reaction can be identified by the presence of the two intense peaks that appear at 3263 and 2895 cm^{-1}, which correspond to the stretching vibration of the O−H bond in NH_2OH and ONH_2OH, respectively.

In Figure 2g, we present the simulated IR spectrum of the products of reaction pathway 6, which are NH_2OH and NH_2OOH. The highest in wavenumber peak is the stretching vibration of the O−O−H bond and O−H, which appears around 3720 cm^{-1} in a moderate intensity peak. At 3543 cm^{-1}, we observe the antisymmetric stretching vibration of the NH_2 group in NH_2OOH, which is somewhat lower in wavenumber than that of NH_2OH. The symmetric stretching frequency of the NH_2 group appears at 3399 cm^{-1} in a moderate-to-intense peak. At 1636 cm^{-1}, we observe the bending motion of the NH_2 group, which is a weak-to-moderate peak. At 1380 cm^{-1}, we observe the bending motion of the O−H group in the two molecules, NH_2OH and NH_2OOH. A doublet at 1168 and 1134 cm^{-1} appears as the bending motion of the NH_2 group of NH_2OH and NH_2OOH, respectively. At 911 cm^{-1}, we have the stretching vibration of the N−O bond in NH_2OH, and at 689 cm^{-1}, the stretching vibration of the O−O bond in NH_2OOH. The last four peaks can be used to identify the products of pathway 6.

We observe that the simulated IR spectra of the products of the 6 reaction pathways can give a clear distinction between the various products formed by ammonia synthesis from water and nitrogen. We anticipate that the calculated results will be helpful to experimental efforts in analyzing reaction mixtures that are formed when water is reacted with nitrogen in plasma-assisted synthesis of nitrogen-containing molecules that could potentially be used as fuels.[43−46]

The implications of the per-oxidized state of nitrogen and their tendency to therefore produce more NO_x (NO, NO_2) and N_2O during the combustion should therefore be further assessed. For this reason, we provide the infrared absorption

Downloaded from pubs.acs.org/acsodf/article-pdf/doi/10.1021/acsomega.6c03586/6768896/acsomega.6c03586.pdf by Constantinos Zeinalipour-Yazdi on 29 August 2026

https://doi.org/10.1021/acsomega.6c03586
ACS Omega XXXX, XXX, XXX−XXX

modes of every possible reaction product in this work. Also, the stability of the oxidized nitrogen-containing compounds should be further evaluated, as these may be potential products in plasma-assisted and other high-energy synthesis methods, which may result in higher N_2O concentrations during their combustion. The reduction of N_2O is critical as it possesses a global warming potential (GWP) 273 times greater than carbon dioxide.

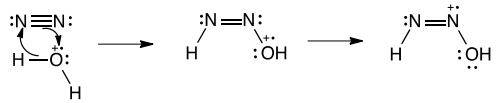
3.3. Proposed Mechanism of Plasma-Induced Ammonia Synthesis from N_2 and H_2O

The balanced chemical equation for ammonia synthesis from water and nitrogen is as follows

$$N_2(g) + 3H_2O(g) \rightarrow 2NH_3(g) + 3/2O_2(g) \quad (12)$$

The relative stoichiometric ratios of N_2/H_2O in this balanced chemical reaction are 1:3, and the similar collisional cross section of N_2 (4.3×10^{-15} cm^2) and H_2O (3.8×10^{-5} cm^2) suggests that it is three times more probable that H_2O will be ionized by energetic electrons in a plasma chamber. Additionally, oxygen has a lower first ionization energy (1314 kJ mol^{-1}) compared to nitrogen, which has a first ionization energy of (IE_1) 1402 kJ mol^{-1}. This suggests that in a mixture of 1:3 of nitrogen and water in the gas phase, it is the water that would mostly ionize by the plasma, forming H_2O^+. This water radical cation can react with nitrogen in the gas mixture, forming the radical cation $[H{-}N = N{-}OH]^+$, according to Scheme 1.

Scheme 1. Proposed Reaction Mechanism Step for the Reaction of H_2O^+ with N_2

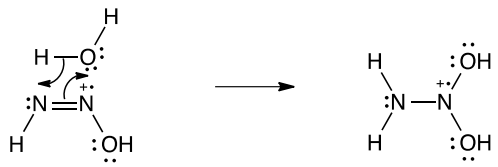


The second step in this reaction mechanism is due to an internal redistribution of electrons to result in a more stable intermediate species, which is mainly attributed to the electronegativity of oxygen (3.44) being greater than the electronegativity of nitrogen (3.04), suggesting that the positive formal charge is more stable on the nearby nitrogen rather than the oxygen of the hydroxyl group. This resonance form of the radical cation $[H{-}N = N{-}OH]^+$ would undergo further reaction with water, as water is the more abundant species in the gas phase, according to the following reaction mechanism step (as shown in Scheme 2).

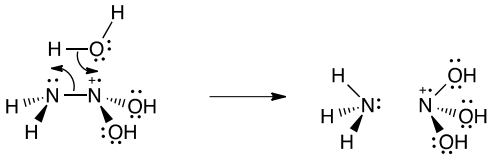
This forms a second radical cation intermediate, $[H_2N{-}N(OH)_2]^+$, that would react further with water molecules due to the higher stoichiometric ratio of water compared to nitrogen. This reaction mechanism step is shown in Scheme 3.

This reaction mechanism step forms the first stoichiometric ammonia molecule and the hydroxylate radical cation $[N(OH)_3]^+$, which is stabilized by the electron-withdrawing character of O, being more electronegative than nitrogen. Nonetheless, as this intermediate is a radical species, it would eventually react with another water molecule, abstracting a hydrogen from it according to Scheme 4, forming trihydroxyammonium cation, $[H{-}N(OH)_3]^+$, and a hydroxyl radical.

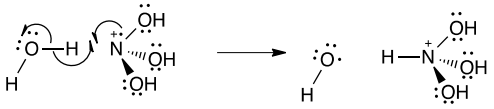
Scheme 2. Proposed Reaction Mechanism Step for the Reaction of $[H{-}N = N{-}OH]^+$ with H_2O



Scheme 3. Proposed Reaction Mechanism Step for the Reaction of $[H{-}N = N{-}OH]^+$ with H_2O

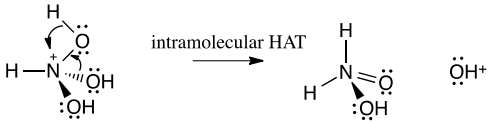


Scheme 4. Proposed Reaction Mechanism Step for the Reaction of $[N(OH)_3]^+$ with H_2O



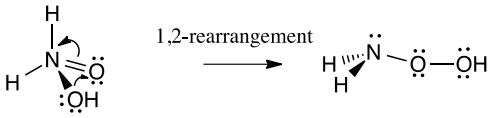
Trihydroxyammonium cation ($HN(OH)_3^+$) would undergo an intramolecular hydrogen atom transfer (HAT), forming ONH_2OH (a new product identified in this work) and a hydroxyl cation (OH^+, oxylium ion), which is a highly reactive intermediate species, as shown in Scheme 5.

Scheme 5. Intramolecular Hydrogen Atom Transfer (HEA) of $HN(OH)_3^+$ Forming ONH_2OH (a New Product Identified in This Work) and a Hydroxyl Cation



This new product resembles the general class of compounds of nitronic acids, which are known to undergo an intramolecular 1,2-rearrangement (oxotropic rearrangement), forming aminohydroperoxide (H_2NOOH) according to Scheme 6, which is the other new product we identified in this work.

Scheme 6. 1,2-Rearrangement of ONH_2OH Forming Aminohydroperoxide (H_2NOOH)



4. CONCLUSIONS

Our computational analysis within density functional theory at the B3LYP/aug-cc-pVDZ level of theory indicates that the synthesis of ammonia and hydrazine from water and nitrogen is highly endothermic ($\Delta H \gg 0$) and decreases in entropy ($\Delta S < 0$), which suggests that it is a nonspontaneous process ($\Delta G > 0$). The Gibbs free energy change for the synthesis of ammonia is 794 kJ·mol^{-1}, which makes it prohibitively endergonic. Any reaction pathway would at least have a barrier of +794 kJ·mol^{-1}. Additionally, the synthesis of

Downloaded from pubs.acs.org/acsodf/article-pdf/doi/10.1021/acsomega.6c03586/6768896/acsomega.6c03586.pdf by Constantinos Zeinalipour-Yazdi on 29 August 2026

https://doi.org/10.1021/acsomega.6c03586
ACS Omega XXXX, XXX, XXX−XXX

hydrazine from N_2 and water is also possible at a Gibbs free energy cost of 713 kJ·mol^{-1}. Other synthetic routes that involve the formation of hydroxylamine (NH_2OH) and ammonia are also very endergonic (ΔG = 786 kJ·mol^{-1}). From our computational analysis, it is evident that many nitrogen-containing fuels can be produced from N_2 and water, and these have different heat contents depending on the degree of oxidation of ammonia. We identify two new molecules, NH_2OOH and ONH_2OH, that are oxidized products of ammonia and have not been previously reported, which could potentially form during the synthesis of ammonia via plasma-assisted methods. The relative stability of these molecules and their existence could be assessed via infrared spectroscopy, where every nitrogen-containing molecule has features that are distinct and identifiable with the use of infrared spectroscopy. We propose a mechanism that explain the formation of these new molecules under plasma conditions.

■ ASSOCIATED CONTENT

Data Availability Statement

Cartesian coordinates of all fully optimized structures reported and data supporting this article are available on ResearchGate with the following DOI: 10.13140/RG.2.2.24198.23368.

■ AUTHOR INFORMATION

Corresponding Author

Constantinos D. Zeinalipour-Yazdi − *Bioscience and Chemistry, Faculty of Computing, Mathematics, Engineering and Natural Sciences, One Portsoken, London E1 8PH, U.K.; Department of Mechanical and Aerospaces, Brunel University London, Uxbridge UB8 3PH, U.K.;* orcid.org/0000-0002-8388-1549; Email: zeinalip@gmail.com, constantinos.zeinalipour@nulondon.ac.uk, c.zeinalipouryazti@northeastern.edu

Author

Xinyan Wang − *Department of Mechanical and Aerospaces, Brunel University London, Uxbridge UB8 3PH, U.K.;* orcid.org/0000-0002-1988-3742

Complete contact information is available at: https://pubs.acs.org/10.1021/acsomega.6c03586

Author Contributions

C.D.Z.-Y.: did the conceptualization, data curation, and investigation of the study and wrote the first original draft. X.W.: Writing—review and editing.

Notes

The authors declare no competing financial interest.

■ ACKNOWLEDGMENTS

C.D.Z.-Y. acknowledges Brunel University London for computational resources for this manuscript and X.W. for an honorary visiting research fellow position.

■ REFERENCES

(1) Kojima, Y.; Yamaguchi, M. Ammonia as a hydrogen energy carrier. *Int. J. Hydrogen Energy* **2022**, *47* (54), 22832−22839.

(2) Garabedian, C. G.; Johnson, J. H. The Theory of Operation of an Ammonia Burning Internal Combustion Engine; US Army Tank-Automotive Center: Michigan, USA, 1965. https://apps.dtic.mil/sti/citations/AD0634681 (accessed May 31, 2021).

(3) Zamfirescu, C.; Dincer, I. Using ammonia as a sustainable fuel. *J. Power Sources* **2008**, *185*, 459−465.

(4) Cinti, G.; Frattini, D.; Jannelli, E.; Desideri, U.; Bidini, G. Coupling Solid Oxide Electrolyser (SOE) and ammonia production plant. *Appl. Energy* **2017**, *192*, 466−476.

(5) Serpell, O.; Hsain, Z.; Chu, A.; Johnsen, W. Ammonia's Role in a Net-Zero Hydrogen Economy; Klainman Center for Energy Policy March, 2023.

(6) The Royal Society. Ammonia: Zero-Carbon Fertilizer, Fuel and Energy Store, 2020. https://royalsociety.org/-/media/policy/projects/green-ammonia/green-ammonia-policybriefing.

(7) Salmon, N.; Bañares-Alcántara, R.; Nayak-Luke, R. Optimization of green ammonia distribution systems for intercontinental energy transport. *iScience* **2021**, *24*, No. 102903.

(8) Zeinalipour-Yazdi, C. D.; Hargreaves, J. S. J.; Laassiri, S.; Catlow, C. R. A. A comparative analysis of the mechanisms of ammonia synthesis on various catalysts using density functional theory. *R. Soc. Open Sci.* **2021**, *8* (11), No. 210952.

(9) Zeinalipour-Yazdi, C. D.; Hargreaves, J. S. J.; Catlow, C. R. A. Nitrogen Activation in a Mars−van Krevelen Mechanism for Ammonia Synthesis on Co3Mo3N. *J. Phys. Chem. C* **2015**, *119* (51), 28368−28376.

(10) Zeinalipour-Yazdi, C. D.; Hargreaves, J. S. J.; Catlow, C. R. A. DFT-D3 Study of Molecular N2 and H2 Activation on Co3Mo3N Surfaces. *J. Phys. Chem. C* **2016**, *120* (38), 21390−21398.

(11) Zeinalipour-Yazdi, C. D.; Hargreaves, J. S. J.; Catlow, C. R. A. Low-T Mechanisms of Ammonia Synthesis on Co3Mo3N. *J. Phys. Chem. C* **2018**, *122*, 6078−6082.

(12) Higham, M. D.; Zeinalipour-Yazdi, C. D.; Hargreaves, J. S. J.; Catlow, C. R. A. Mechanism of ammonia synthesis on Fe3Mo3N. *Faraday Discuss.* **2023**, *243*, 77−96.

(13) Laassiri, S.; Zeinalipour-Yazdi, C. D.; Catlow, C. R. A.; Hargreaves, J. S. J. The potential of manganese nitride based materials as nitrogen transfer reagents for nitrogen chemical looping. *Appl. Catal., B* **2018**, *223*, 60−66.

(14) Ertl, G.; Knözinger, H.; Weitkamp, J. *Handbook of Heterogeneous Catalysis*; VCH: Weinheim, 1997; Vol. 2.

(15) O'Neill, R. P.; Weber, A. Z.; Jacobson, D. L. Steam Methane Reforming: Thermodynamics and Kinetics. *Catal. Rev.* **2009**, *51* (2), 293−325.

(16) Keith, J. A.; Herron, W. D. Water-gas shift reaction: Finding the mechanistic boundary. *Surf. Sci.* **2009**, *603* (8−10), 1335−1343.

(17) Chen, S.; Perathoner, S.; Ampelli, C.; Centi, G. Electrochemical Dinitrogen Activation: To Find a Sustainable Way to Produce Ammonia. In *Studies in Surface Science and Catalysis*; Albonetti, S.; Perathoner, S.; Quadrelli, E. A., Eds.; Elsevier, 2019; Chapter 2, Vol. *178*, pp 31−46.

(18) Erisman, J. W.; Sutton, M. A.; Galloway, J.; Klimont, Z.; Winiwarter, W. How a century of ammonia synthesis changed the world. *Nat. Geosci.* **2008**, *1*, 636.

(19) Rosser, J. M.; Mohtadi, R. S.; Keith, J. M. Renewable Hydrogen: Potential Pathways for Ammonia Production. *Joule* **2018**, *2* (2), 270−292.

(20) Chen, Y.; Otsuka, K.; Wan, X.; Oh, J. H.; Kim, J. H.; Wei, K.-H. Solution-Processed Graphene-Based Transparent Conductive Films for Organic Photovoltaic Devices. *Org. Electron.* **2012**, *13* (1), 49−55.

(21) Awan, H.; Feng, K.; Yu, J.; Zheng, Y.; Hu, L. Emerging Semitransparent Solar Cells: Materials and Device Design. *Adv. Energy Mater.* **2018**, *8* (17), No. 1703439.

(22) Boningari, T.; Smirniotis, P. G. Impact of nitrogen oxides on the environment and human health: Mn-based materials for the NOx abatement. *Curr. Opin. Chem. Eng.* **2016**, *13*, 133−141.

(23) Bosch, H.; Janssen, F. J. J. G. Formation and control of nitrogen oxides. *Catal. Today* **1988**, *2* (4), 369−379.

(24) Tomašić, V. Application of the monoliths in DeNOx catalysis. *Catal. Today* **2007**, *119* (1), 106−113.

(25) Park, T. S.; Jeong, S. K.; Hong, S. H.; Hong, S. C. Selective Catalytic Reduction of Nitrogen Oxides with NH3 over Natural

Downloaded from pubs.acs.org/acsodf/article-pdf/doi/10.1021/acsomega.6c03586/6768896/acsomega.6c03586.pdf by Constantinos Zeinalipour-Yazdi on 29 August 2026

Manganese Ore at Low Temperature. *Ind. Eng. Chem. Res.* **2001**, *40* (21), 4491−4495.
(26) Han, L.; Cai, S.; Gao, M.; Hasegawa, J.-Y.; Wang, P.; Zhang, J.; Shi, L.; Zhang, D. Selective Catalytic Reduction of NOx with NH3 by Using Novel Catalysts: State of the Art and Future Prospects. *Chem. Rev.* **2019**, *119* (19), 10916−10976.
(27) Song, X.; Basheer, C.; Zare, R. N. Making ammonia from nitrogen and water microdroplets. *Proc. Natl. Acad. Sci. U.S.A.* **2023**, *120* (16), No. e2301206120.
(28) Lan, R.; Irvine, J. T. S.; Tao, S. Synthesis of ammonia directly from air and water at ambient temperature and pressure. *Sci. Rep.* **2013**, *3* (1), No. 1145.
(29) Wu, H.; Yang, L.; Wen, J.; Xu, Y.; Cai, Y.; Gao, W.; Wang, Q.; Guan, Y.; Feng, S.; Cao, H.; He, T.; Liu, L.; Zhang, S.; Guo, J.; Chen, P. Plasma-Driven Nitrogen Fixation on Sodium Hydride. *Adv. Energy Mater.* **2023**, *13* (27), No. 2300722.
(30) Bogaerts, A.; Neyts, E. C. Plasma Technology: An Emerging Technology for Energy Storage. *ACS Energy Lett.* **2018**, *3* (4), 1013−1027.
(31) Hong, J.; Prawer, S.; Murphy, A. B. Plasma Catalysis as an Alternative Route for Ammonia Production: Status, Mechanisms, and Prospects for Progress. *ACS Sustainable Chem. Eng.* **2018**, *6* (1), 15−31.
(32) Mehta, P.; Barboun, P.; Go, D. B.; Hicks, J. C.; Schneider, W. F. Catalysis Enabled by Plasma Activation of Strong Chemical Bonds: A Review. *ACS Energy Lett.* **2019**, *4* (5), 1115−1133.
(33) Mehta, P.; Barboun, P. M.; Engelmann, Y.; Go, D. B.; Bogaerts, A.; Schneider, W. F.; Hicks, J. C. Plasma-Catalytic Ammonia Synthesis beyond the Equilibrium Limit. *ACS Catal.* **2020**, *10* (12), 6726−6734.
(34) Mehta, P.; Barboun, P.; Herrera, F. A.; Kim, J.; Rumbach, P.; Go, D. B.; Hicks, J. C.; Schneider, W. F. Overcoming ammonia synthesis scaling relations with plasma-enabled catalysis. *Nat. Catal.* **2018**, *1* (4), 269−275.
(35) Wang, Y.; Craven, M.; Yu, X.; Ding, J.; Bryant, P.; Huang, J.; Tu, X. Plasma-Enhanced Catalytic Synthesis of Ammonia over a Ni/Al2O3 Catalyst at Near-Room Temperature: Insights into the Importance of the Catalyst Surface on the Reaction Mechanism. *ACS Catal.* **2019**, *9* (12), 10780−10793.
(36) Wang, Y.; Yang, W.; Xu, S.; Zhao, S.; Chen, G.; Weidenkaff, A.; Hardacre, C.; Fan, X.; Huang, J.; Tu, X. Shielding Protection by Mesoporous Catalysts for Improving Plasma-Catalytic Ambient Ammonia Synthesis. *J. Am. Chem. Soc.* **2022**, *144* (27), 12020−12031.
(37) Dunning, T. H., Jr. Gaussian basis sets for use in correlated molecular calculations. I. The atoms boron through neon and hydrogen. *J. Chem. Phys.* **1989**, *90*, 1007−1023.
(38) Becke, A. D. Density-Functional Thermochemistry. III. The Role of Exact Exchange. *J. Chem. Phys.* **1993**, *98*, 5648.
(39) Lee, C.; Yang, W.; Parr, R. G. Development of the Colle-Salvetti correlation-energy formula into a functional of the electron density. *Phys. Rev. B* **1988**, *37*, No. 785.
(40) Frisch, M. J.; Trucks, G. W.; Schlegel, H. B.; Scuseria, G. E.; Robb, M. A.; Cheeseman, J. R.; Scalmani, G.; Barone, V.; Petersson, G. A.; Nakatsuji, H.; Li, X.; Caricato, M.; Marenich, A. V.; Bloino, J.; Janesko, B. G.; Gomperts, R.; Mennucci, B.; Hratchian, H. P.; Ortiz, J. V.; Izmaylov, A. F.; Sonnenberg, J. L.; Williams-Young, D.; Ding, F.; Lipparini, F.; Egidi, F.; Goings, J.; Peng, B.; Petrone, A.; Henderson, T.; Ranasinghe, D.; Zakrzewski, V. G.; Gao, J.; Rega, N.; Zheng, G.; Liang, W.; Hada, M.; Ehara, M.; Toyota, K.; Fukuda, R.; Hasegawa, J.; Ishida, M.; Nakajima, T.; Honda, Y.; Kitao, O.; Nakai, H.; Vreven, T.; Throssell, K.; Montgomery, J. A., Jr.; Peralta, J. E.; Ogliaro, F.; Bearpark, M. J.; Heyd, J. J.; Brothers, E. N.; Kudin, K. N.; Staroverov, V. N.; Keith, T. A.; Kobayashi, R.; Normand, J.; Raghavachari, K.; Rendell, A. P.; Burant, J. C.; Iyengar, S. S.; Tomasi, J.; Cossi, M.; Millam, J. M.; Klene, M.; Adamo, C.; Cammi, R.; Ochterski, J. W.; Martin, R. L.; Morokuma, K.; Farkas, O.; Foresman, J. B.; Fox, D. J. *Gaussian 16*, revision C.01; Gaussian, Inc.: Wallingford, CT, 2016.
(41) Zeinalipour-Yazdi, C. D.; Catlow, C. R. A. A Computational Study of the Heterogeneous Synthesis of Hydrazine on Co3Mo3N. *Catal. Lett.* **2017**, *147* (7), 1820−1826.
(42) Gilbert, T. R.; Kirss, R. V.; Bretz, S. L.; Foster, N. *Chemistry: The Science in Context*, 6th ed.; W.W. Norton & Company, 2020.
(43) Zhang, T.; Zhou, R.; Zhang, S.; Zhou, R.; Ding, J.; Li, F.; Hong, J.; Dou, L.; Shao, T.; Murphy, A. B.; Ostrikov, K.; Cullen, P. J. Sustainable Ammonia Synthesis from Nitrogen and Water by One-Step Plasma Catalysis. *Energy Environ. Mater.* **2023**, *6* (2), No. e12344.
(44) Hawtof, R.; Ghosh, S.; Guarr, E.; Xu, C.; Mohan Sankaran, R.; Renner, J. N. Catalyst-free, highly selective synthesis of ammonia from nitrogen and water by a plasma electrolytic system. *Sci. Adv.* **2019**, *5* (1), No. eaat5778.
(45) Song, S.; Wang, F.; Sun, X.; Chen, Y.; Liu, J.; Shi, Y.; Ning, P.; Ma, Y.; Li, K. Plasma-Assisted Ammonia Synthesis from N2 and H2O over rGO-TiO2 Catalysts: Enhancing Energy Efficiency and Unraveling Reaction Mechanisms. *ACS Catal.* **2025**, *15* (20), 17603−17613.
(46) Zhang, J.; Li, X.; Zheng, J.; Du, M.; Wu, X.; Song, J.; Cheng, C.; Li, T.; Yang, W. Non-thermal plasma-assisted ammonia production: A review. *Energy Convers. Manage.* **2023**, *293*, No. 117482.

Downloaded from pubs.acs.org/acsodf/article-pdf/doi/10.1021/acsomega.6c03586/6768896/acsomega.6c03586.pdf by Constantinos Zeinalipour-Yazdi on 29 August 2026

https://doi.org/10.1021/acsomega.6c03586
ACS Omega XXXX, XXX, XXX−XXX